The QCAD Framework for Quantum Device Modeling

X. Gao, E. Nielsen, R. P. Muller, R. W. Young, A. G. Salinger, N. C. Bishop, and M. S. Carroll
Sandia National Laboratories
1515 Eubank SE, Albuquerque, NM 87123, USA
e-mail: xngao@sandia.gov, enielse@sandia.gov, rmuller@sandia.gov

***Abstract*— We present the Quantum Computer Aided Design (QCAD) simulator that targets modeling quantum devices, particularly Si double quantum dots (DQDs) developed for quantum computing. The simulator core includes Poisson, Schrodinger, and Configuration Interaction solvers which can be run individually or combined self-consistently. The simulator is built upon Sandia-developed Trilinos and Albany components, and is interfaced with the Dakota optimization tool. It is being developed for seamless integration, high flexibility and throughput, and is intended to be open source. The QCAD tool has been used to simulate a large number of fabricated silicon DQDs and has provided fast feedback for design comparison and optimization.**

Keywords— QCAD, Quantum devices, DQDs, qubit, Optimization

I. Introduction

Semiconductor quantum dots for quantum information processing have shown remarkable progress [1], [2] in recent years. Sandia National Laboratories has been involved [3] in an effort that uses Si-based DQD qubits for quantum computing. A physics-based robust simulator capable of quantum device modeling is vital to facilitate the experimental development of this technology. There are a number of challenges associated with modeling realistic DQDs, i.e., the need to handle complex geometries, many different device layouts, convergence at low temperatures, and 3D quantum effects. Existing commercial and academic TCAD tools often handle one or two of these challenges but not all of them. The Sandia Quantum Computer Aided Design (QCAD) project is developing an integrated tool that aims at addressing these challenges to analyze and advance designs of DQDs used as qubits, leveraging a number of Sandia-developed software programs [4] including the Trilinos suite, the Albany code, the Dakota toolbox, and the Cubit geometry and meshing tool.

In this paper, we present the QCAD device simulator whose core includes Poisson, Schrodinger, and Configuration Interaction (CI) solvers. It is built upon the Trilinos and Albany projects, and is interfaced with the Dakota toolbox. The simulator is developed such that all components work together seamlessly (high integration), and all core solvers can be run individually or self-consistently for 1D/2D/3D quantum devices made from multiple different materials (high flexibility), while allowing high simulation throughput due to distributed parallelization and scripting. We intend to make the code open source once it reaches maturity. By using the QCAD simulator, we have been able to perform a large number of simulations for many experimental DQDs, and have provided fast feedback regarding which device layouts are more likely to lead to few-electron behavior (critical for qubit operation). We can also investigate quantum confinement effects on device characteristics with the quantum solvers.

The QCAD framework and its core solvers are described in Section II. Some simulation results of quantum dots are shown in Section III demonstrating usage of the QCAD simulator, followed by a summary in Section V.

II. The QCAD Framework

The QCAD software framework is given in Fig. 1. The base of the framework is Trilinos [4], an open-source suite consisting of mathematical libraries (nonlinear and linear solvers, preconditioners, eigensolvers, etc.), discretization utilities, an automatic differentiation library, distributed parallel toolkits, and many more packages (refer to

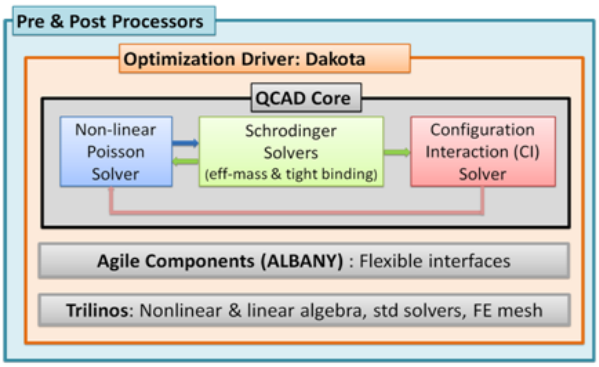

Fig. 1. Diagram of the QCAD software framework

trilinos.sandia.gov for details). The Albany code provide a unified and flexible interface to those Trilinos packages to minimize the coding effort for users developing physical models.

The QCAD core contains nonlinear Poisson (P), effective-mass Schrodinger (S), and CI solvers. These solvers can be run individually or combined in a self-consistent manner. The Poisson and Schrodinger solvers can be coupled self-consistently to obtain single-particle envelope wave functions and energy levels. The P-S solution can be used as an eigenbasis for the CI solver which is then coupled with the Poisson solver. This self-consistent P-S-CI description produces the accurate many-particle wave functions and energies within the effective mass approximation, which are important in quantitative study of few-electron DQD behavior. Some details about the Poisson, Schrodinger, and self-consistent P-S solvers are described in the following subsections, while the self-consistent P-S-CI description will be given elsewhere, and the CI method can be found in Ref. [5].

Outside the QCAD core is the Dakota driver which repeatedly calls the QCAD executable to perform specified optimization tasks. Dakota [4] is an open-source tool which provides nonlinear least square optimization, parameter studies, and uncertainty quantification.

A. Poisson and Schrodinger Solvers

The well-known Poisson equation in a semiconductor is given by

$$-\nabla(\epsilon_s \nabla\phi) = q[p(\phi) - n(\phi) + N_D^+(\phi) - N_A^-(\phi)]. \quad (1)$$

The hole and electron concentrations, $p(\phi)$ and $n(\phi)$, are related to the electrostatic potential ϕ through carrier statistics. Both Maxwell-Boltzmann and Fermi-Dirac statistics are implemented in QCAD. At low temperatures (below $4\,\mathrm{K}$) the incomplete ionization of dopants is incorporated [6] by including only the ionized concentrations on the right-hand-side of (1).

The equation is discretized by the finite element method and solved by the Newton nonlinear solver embedded in Trilinos. Three types of boundary conditions are considered [6], i.e., flux conservation between different materials (continuity of $\epsilon_s \nabla\phi \cdot \mathbf{n}$ across material interfaces), Neumann, and Dirichlet conditions. This nonlinear Poisson solver provides a semiclassical Thomas-Fermi description of the electrostatics in quantum devices which in many cases has proven sufficient to understand the behavior of real DQDs.

The time-independent effective mass Schrodinger equation takes the form of

$$\frac{-\hbar^2}{2}\nabla\left(\frac{1}{m^*}\nabla\psi_i\right) + V\psi_i = E_i\psi_i. \quad (2)$$

The Schrodinger equation is discretized by the finite element approach and the resulting eigenvalue problem is solved using a Trilinos eigensolver package called Anasazi. The equation is solved with closed boundary conditions, i.e., $\psi = 0$ on Dirichlet boundaries, $\frac{1}{m^*}\nabla\psi \cdot \mathbf{n} = 0$ on Neumann boundaries, and $\frac{1}{m^*}\nabla\psi \cdot \mathbf{n}$ is continuous across material interfaces.

B. Self-Consistent Poisson-Schrodinger Solver

In realistic quantum devices such as DQDs, we can divide the entire structure (relatively large) into semiclassical and quantum regions. In semiclassical regions, solving the nonlinear Poisson equation alone is often sufficient; whereas in quantum regions, the Poisson and Schrodinger equations need to be coupled self-consistently for electrons (we focus on electrons only as they are used for qubit operation).

To couple the two equations, the electron concentration $n(\phi)$ in (1) becomes $n(\phi, E_i, \psi_i)$, where E_i is the ith eigen-energy and ψ_i is the corresponding ith envelop wave function. The general expression is given by $n(\phi, E_i, \psi_i) = \sum_i N_i|\psi_i|^2$, where the N_i term takes different expressions depending on confinement dimensionality [6].

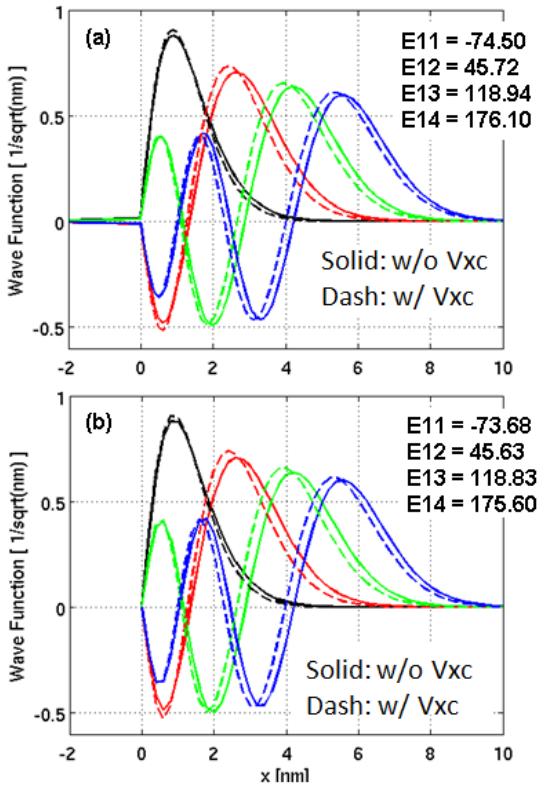

Fig. 2. Δ_2-valley lowest four subband wave functions and energies in a 1D MOS capacitor at T = 50 K and Vg = 3 V obtained from QCAD (a) and from SCHRED (b). The solid and dashed curves are obtained without and with the exchange-correlation effect, respectively. Also shown are the subband energies in [meV] (referred to Fermi level) with the exchange-correlation effect.

The potential energy V in (2) becomes a function of ϕ and n and takes the following form,

$$V(\phi, n) = E_{ref} - \chi - q\phi + V_{xc}(n), \qquad (3)$$

where E_{ref} is a constant reference energy, χ is electron affinity, and $V_{xc}(n)$ is the exchange-correlation correction due to Pauli exclusion principle in real many-electron systems. For the $V_{xc}(n)$ term, we implemented the well-known parameterized expression by Hedin and Lundqvist [7].

The self-consistency of the two equations is achieved by using an efficient predictor-corrector scheme [8]. This scheme is extended [6] to any 1D/2D/3D-confined quantum structure. The self-consistent P-S solver currently solves the conduction Δ_2-valleys only in silicon devices (whose principle axis is perpendicular to the Si/SiO2 interface)

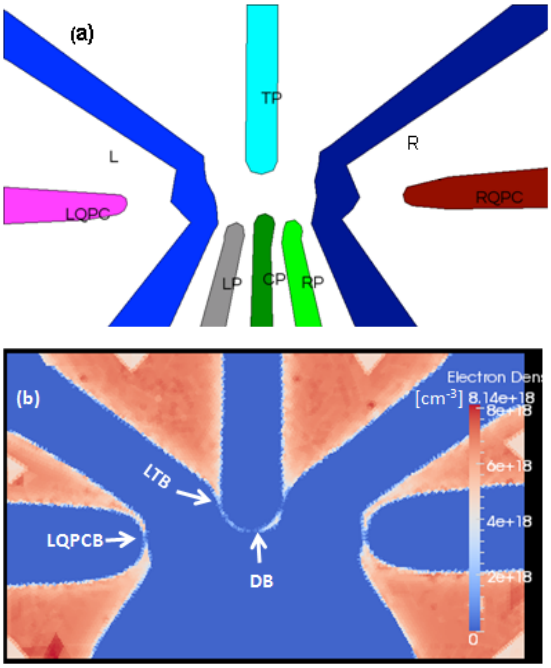

Fig. 3. (a) Top view of the depletion gate pattern in a Si DQD. (b) Top view of electron density at the Si/SiO2 interface (T = 0.2 K). The gate voltages that meet the optimization targets are AG = 3.48 V, TP = -0.74 V, CP = -0.007 V, LP = RP = -5.95 V, L = R = -1.15 V, LQPC = RQPC = -2.41 V.

due to their lower energy and the targeted low-temperature applications.

To validate the P-S solver, we performed simulations on a 1D MOS capacitor with 4-nm oxide and 5e17 cm^{-3} p-substrate doping. The Δ_2-valley lowest four wave functions and energies in the capacitor between QCAD and SCHRED [9] are compared in Fig. 2. The results produced by the two tools show excellent agreement.

III. Application of QCAD Simulator

The Dakota driver component of QCAD (compiled into the QCAD executable) enables optimization of gate voltages for simultaneous targets that are likely to lead to few-electron quantum dots. Fig. 3(a) shows a top view of the polysilicon depletion gate pattern (transferred from a SEM image) in an experimental Si DQD. Fig. 3(b) shows a top view of the electron density at the Si/SiO2 interface under one optimization scenario, where the depletion gates (TP, CP, LP tied to RP, L tied to R, LQPC tied to RQPC) and top Aluminum gate AG (not shown) voltages are allowed to vary, so as to obtain one

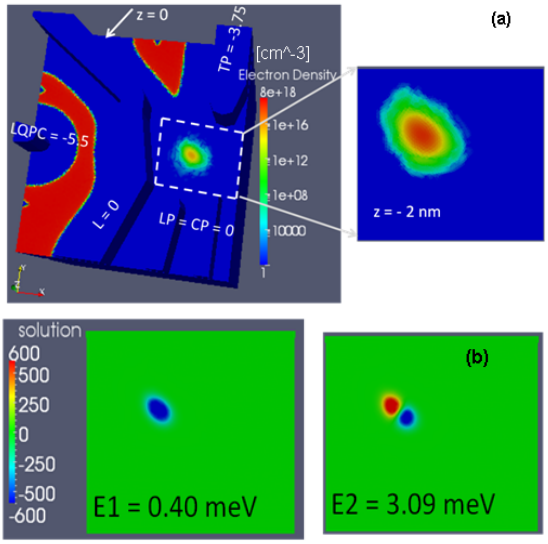

Fig. 4. (a) Electron density in a Si single quantum dot at T = 4 K obtained from the self-consistent Poisson-Schrodinger solver. The indicated voltages are experiment operating values. The z = 0 surface is the Si/SiO2 interface where the interface charge is used as a tuning parameter to obtain integrated electron density equal to one. The dash white box denotes the quantum region where the self-consistent solver is applied and the semiclassical Poisson solver is used in the rest of the device. Also shown is the electron density in the z = -2 nm surface where it shows peak values. (b) The lowest two wave functions and energies (referred to Fermi level) in the quantum dot at the z = -2 nm surface.

electron (integrated electron density close to one) in the left dot and simultaneously turn on the left tunnel barrier (LTB in the figure), dot barrier (DB), and left QPC barrier (LQPCB). The gate voltages that meet these optimization targets are given in the caption of Fig. 3. Locations of tunnel barriers (LTB, DB, LQPCB, etc.) are dynamically detected through saddle-point-searching algorithm similar to the Nudged Elastic Band approach [10].

We have performed optimization simulations on dozens of existing (fabricated) and proposed DQD designs. These optimizations have been able to help answer three DQD design questions that are critical in achieving few-electron DQD behavior: (i) which devices allow one electron in each dot and also simultaneous control of tunnel barriers; (ii) for a given device, do tunnel barriers turn on before or after a dot has many electrons; (iii) what are the location and shape of the main dots and charge sensing constrictions.

Using the self-consistent quantum models developed in QCAD, we can investigate effects of spatial confinement in quantum devices. Fig. 4 shows the electron density and wave functions in a Si single quantum dot obtained from the self-consistent P-S solver. It is seen that electron density peak is shifted by about 2 nm away from the Si/SiO2 interface due to spatial confinement and the electron is confined in the dot region.

IV. Conclusion

In summary, we have described the development of the QCAD program that has become a versatile tool for simulating multi-dimensional quantum devices. QCAD simulations of realistic DQDs allow fast and valuable feedback to accelerate the experimental development of few-electron quantum dots.

This work was supported by the Laboratory Directed Research and Development program at Sandia National Laboratories. Sandia is a multiprogram laboratory operated by Sandia Corporation, a Lockheed Martin Company, for the United States Department of Energy's National Nuclear Security Administration under Contract DE-AC04-94AL85000.

References

[1] A. Morello, J. J. Pla, et al., *Single-shot readout of an electron spin in silicon*, Nature **467**, 687 (2010).
[2] M. D. Shulman, O. E. Dial, et al., *Demonstration of entanglement of electrostatically coupled singlet-triple qubits*, Science **336**, 202 (2012).
[3] T. M. Lu, N. C. Bishop, et al., *Enhancement-mode buried strained silicon channel quantum dot with tunable lateral geometry*, Appl. Phys. Lett. **99**, 043101 (2011).
[4] http://trilinos.sandia.gov, http://dakota.sandia.gov, and http://cubit.sandia.gov.
[5] E. Nielsen and R. P. Muller, *A configuration interaction analysis of exchange in double quantum dots*, arXiv:1006.2735 (2010).
[6] X. Gao, E. Nielsen, et al., *in preparation*.
[7] L. Hedin and B. I. Lundqvist, *Explicit local exchange-correlation potentials*, J. Phys. C: Solid Stae Phys. **4**, 2064 (1971).
[8] A. Trellakis, A. T. Galick, A. Pacelli, and U. Ravaioli, *Iteration scheme for the solution of the two-dimensional Schrodinger-Poisson equations in quantum structures*, J. Appl. Phys. **81**, 7880 (1997).
[9] https://nanohub.org/tools/schred.
[10] G. Henkelman, B. P. Uberuaga, and H. Jnsson, *A climbing image nudged elastic band method for finding saddle points and minimum energy paths*, J. Chem. Phys. **113**, 9901 (2000).